“Build your own” ADC mimics: Identification of non-toxic linker/payload mimics for HIC-based DAR determination, high-throughput optimization, and continuous flow conjugation

Marion H. Emmert*+, Cecilia Bottecchia*+, Rodell Barrientos#, Yinnian Feng+, Daniel Holland-Moritz+, Greg Hughes+, Yu-Hong Lam§, Erik Regalado#, Serge Ruccolo+, Shuwen Sun#, Rebecca Chmielowski+, Cuixian Yang+, François Lévesque+

+Process Research & Development (PRD), MRL, Merck & Co., Inc., Rahway, NJ, 07065, USA

#Analytical Research & Development, MRL, Merck & Co., Inc., Rahway, NJ, 07065, USA

§Modeling & Informatics, MRL, Merck & Co., Inc., Rahway, NJ, 07065, USA

KEYWORDS: Maleimide conjugation, high-throughput experimentation, HIC chromatography, microfluidics, continuous flow

ABSTRACT: This manuscript reports the identification of hydrophobic interaction chromatography (HIC)-shifting, non-toxic linker-payload surrogates as tool molecules for the optimization of maleimide/cysteine conjugations relevant to antibody-drug conjugates (ADCs). These tool molecules are demonstrated to allow conjugation measurement *via* HIC with a mAb (monoclonal antibody) bearing engineered cysteines, and for conjugation to mAb interchain cysteines. The linker/payload (LP) mimics were employed to optimize conjugations via high-throughput experimentation and employed to facilitate the development of continuous flow conjugations in a microfluidic reactor and on larger scale. Putative identification of the novel ADC mimics by HIC was confirmed by mass spectrometry. Overall, our studies provide confidence that commercially available, non-toxic LP mimics can be employed successfully to optimize ADC-type conjugations in batch and flow, while minimizing materials needs and experimental work in specialized facilities required for potent compound handling.

Introduction

Antibody-Drug Conjugates (ADCs) are among the fastest growing drug modalities.[1,2] ADCs combine monoclonal antibodies (mAbs) generally targeting specific antigens, such as cancer tissues, with cytotoxic payloads[3-5] and have led to significantly increased survival rates for cancer patients.[6,7] For process development of ADCs, the cytotoxic nature of the linker/payloads (LPs) is a challenge.[8] Since scientists' exposure to these toxic compounds needs to be minimized below specific thresholds,[9] experimental work is often confined to specifically designed laboratories. Establishing such spaces is costly and requires significant capital investment and the associated work in isolators is cumbersome. Overall, the type of equipment that can be brought into and stored in such laboratories is severely constrained, which limits the number of studies that are typically performed to inform on process parameters of the conjugation step (i.e. the last synthetic step) and all subsequent steps of the ADC drug substance process. Importantly, one key technique of process development, the use of high-throughput experimentation,[10] is rarely employed for optimizing ADC conjugations.

To address this challenge, we were inspired by the use of commercially available, non-toxic ADC mimics for analytical development, which have been used extensively in the literature.[11-14] The idea behind these model ADCs is simple, but compelling: since the payload is non-toxic, ADC mimics enable safer and more rapid development of analytical methods. Transferring this principle to conjugation process development would require identifying LP mimics that (i) are non-toxic; (ii) react similarly to actual linker-payloads in conjugation; and (iii) enable the use of established analytical methods for conjugation analysis. Since analytical hydrophobic interaction chromatography (HIC) is often considered the gold standard for determining an ADC's drug-to-antibody ratio (DAR; a key quality attribute of ADCs),[15-20] we focused our efforts on identifying linkers that mimic HIC shifts of the commonly used Monomethyl Auristatin E (MMAE) payload.[1] Herein, we report the identification of HIC-shifting LP mimics (Scheme 1) that allow HIC detection of maleimide conjugation to both engineered[21-23] and interchain[24,25] cysteines.

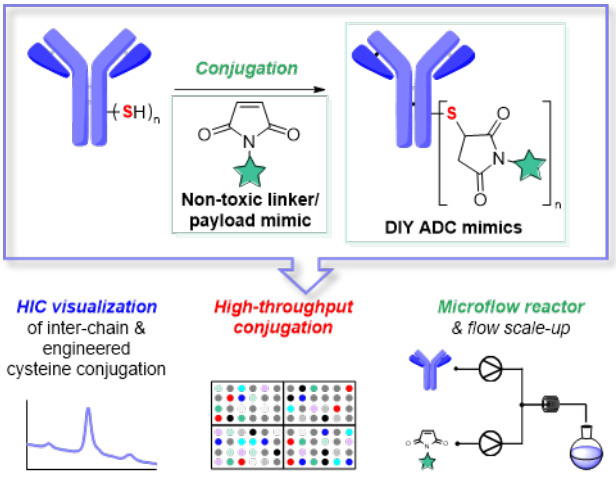

Scheme 1. Linker/Payload mimics for synthesis of custom ADC mimics and continuous flow conjugation development.

These LP mimics were employed in high-throughput conjugation optimization and then leveraged to accelerate the development of continuous flow conjugations. Overall, these studies demonstrate that commercially available, non-toxic LP mimics can be employed to optimize conjugation reactions.

Results and Discussion

Assembling a targeted maleimide collection. To identify suitable LP mimics, we began our investigation by testing a small collection of commonly available maleimides. These maleimides (Scheme 2, bottom) were reacted with a mAb containing two engineered cysteine residues available for conjugation (target DAR2). To assess conjugation between the mAb with engineered cysteines and the first set of 8 maleimides, a HIC method (see the SI for details) with a NH_4OAc salt gradient was employed. HIC traces obtained after 1 h of reaction time are shown in Scheme 2 (top). Unfortunately, no significant shifts in retention time compared to the DAR0 (not conjugated) mAb were observed. This suggests that none of the maleimides tested (**MAL-1** to **MAL-8**) are suitable LP mimics.

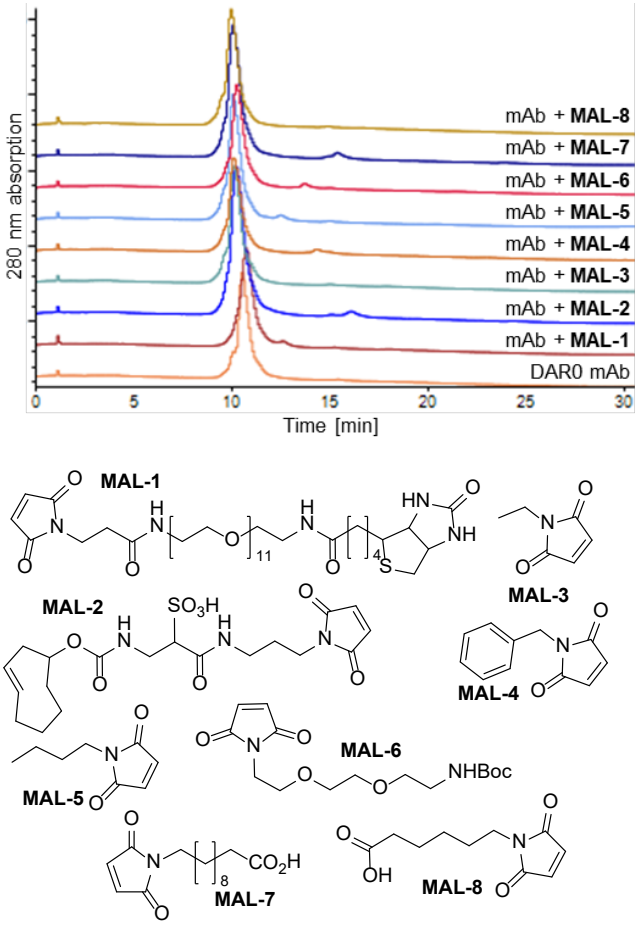

Scheme 2. HIC chromatograms of conjugation reactions between a mAb with 2 engineered free cysteines and MAL-1 through MAL-8. Conditions: 1 h, room temperature (17-22°C), 4 equiv maleimides, 10 mM histidine pH 5.5, 15 g/L mAb.

Based on these data, we focused our efforts on higher throughput testing of maleimide structures, providing the best chance to identify HIC-shifting LP mimics. Our approach to building a large collection of maleimides is visualized in Scheme 3 (for further details, see the SI). With this workflow, >90 compounds were assembled, which are available within our company for conjugation screening.

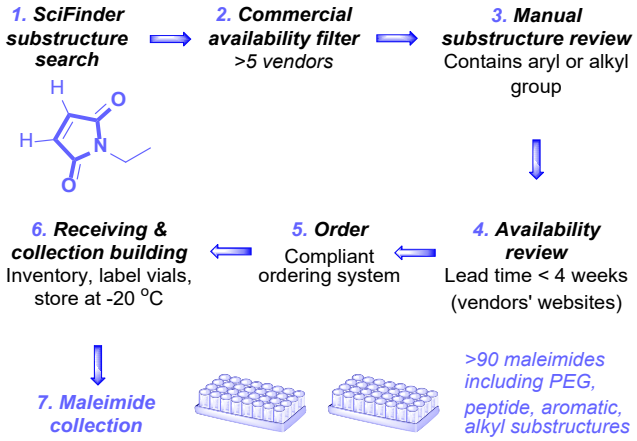

Scheme 3. Building a maleimide collection for high-throughput screening: Workflow and filter rules. Bolded bonds in the structure prevent hits that have annulated rings.

Assessment of maleimide collection. With the maleimide collection in hand, conjugation to the mAb with two engineered cysteine residues (target DAR 2) was re-tested. Reactions were sampled after 1 h and 18 h to allow assessment of short-term and long-term reactivity and to detect potential unclean reactivity or decomposition. Analysis was performed via HIC chromatography after dilution with pH 5.5 histidine buffer and cooling to 5 °C (for further details, see the experimental section and the SI). No significant changes were obtained between the two different time points; therefore, only 1 h data are shown for the purpose of the discussion here (18 h data are provided in the SI). Several of the tested maleimides resulted in significant shifts in the HIC assay, indicating their potential utility as LP mimics. Scheme 4 compares HIC traces of the non-conjugated mAb (D) with the conjugates of a strongly shifting maleimide (E), a weakly shifting LP mimic (C), a non-shifting maleimide (B), and a maleimide that results in the appearance of multiple broad, non-resolved peaks (A). The latter could be indicative of the formation of multiple mAb conjugates, for example via secondary reactivity of moieties on a non-inert maleimide; however, no further studies to identify the reaction products in Scheme 4A were performed.

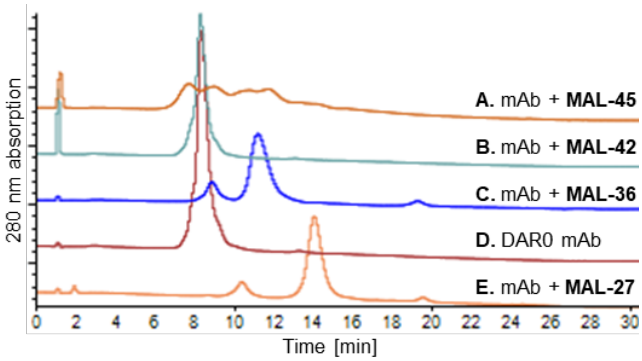

Scheme 4. Examples of HIC chromatograms obtained from evaluating maleimide collection via conjugation. A. Decomposition (**MAL-45**); B. No shift (**MAL-42**); C. Small shift (**MAL-36**); D. decapped mAb starting material; E. Large shift (**MAL-27**). Conditions: 1 h, room temperature, 4 equiv maleimides, 10 mM histidine pH 5.5, 15 g/L mAb.

Table 1. Top maleimides.

Name	HIC shift DAR0 to DAR2	CAS	Synonyms
MAL-27	5.2 min	n/a	N-(Mal-PEG6)-N-bis(PEG3-Boc)
MAL-75	2.3 min	2128735-27-1	N-Mal-N-bis(PEG4-NH-Boc)
MAL-78	2.3 min	1613382-10-7	Maleimido-mono-amide-DOTA-tris (t-Bu ester)
MAL-82	3.3 min	2141976-33-0	endo-BCN-PEG3-mal
MAL-83	4.9 min	756487-18-0	Mc-Phe-Lys(Boc)-PAB
MAL-85	2.1 min	19735-68-3	1-[4-(6-methylbenzothiazol-2-yl)phenyl]pyrrole-2,5-dione
MAL-97	2.8 min	1609659-01-9	TCO-PEG(3)-maleimide

Selection of top maleimides. Based on the result obtained, we selected the most promising maleimides to be used as LP mimics in follow-up studies (Table 1 and Scheme 5). All of the top maleimides exhibit the following features: (i) They show significant shifts (i.e. >2 min) in the employed HIC method (30 min run time); (ii) they are commercially available; (iii) they show 2 distinct peaks in HIC analysis that can be assigned to DAR1 and DAR2 species respectively.

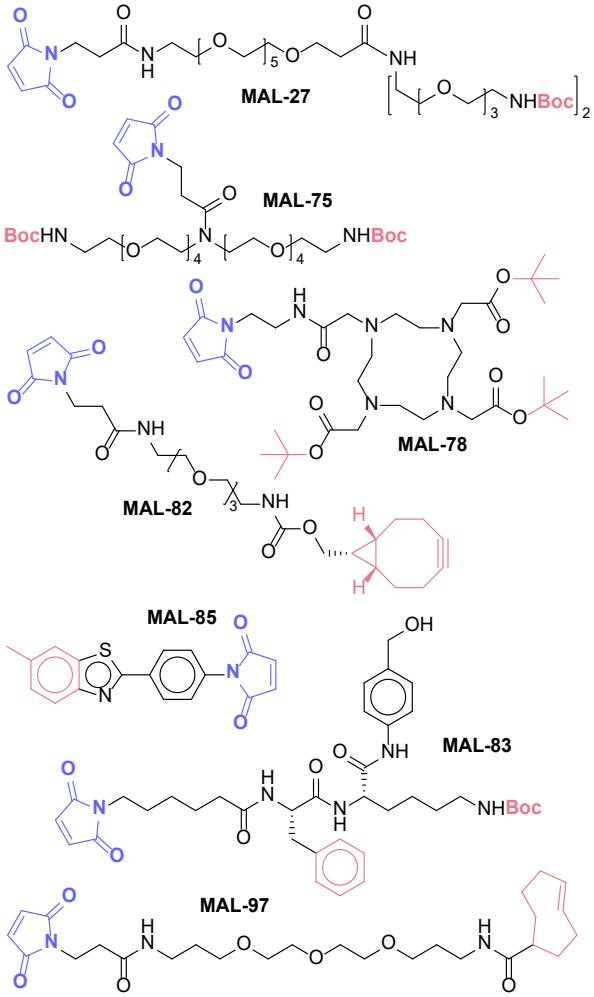

Scheme 5. Structures of top maleimides. Key HIC-shifting substructures are shown in red, while the maleimide handle for conjugation is shown in blue.

From a structural standpoint, all of the top maleimides exhibit hydrophobic groups (Boc, ^{t}Bu, aryl, cyclooctyne/BCN, cyclooctene/TCO; highlighted in red in Scheme 5) in remote positions from the maleimide connecting group (highlighted in blue), which would be pointing away from the linkage site (maleimide) in aqueous solution. This common design concept likely enables good interactions between the hydrophobic substructures and the hydrophobic stationary phase used in the HIC assay. Some of these linkers (**MAL-82** & **MAL-97**) have the potential to not only be used for conjugation, but also provide a handle for further functionalization after conjugation: The cyclo-octyne functionality in **MAL-82** and the trans-cyclooctadiene group in **MAL-97** are both primed for subsequent modifications via click chemistry.[26,27]

SEC and MS analysis for selected DAR2 conjugates. To confirm the structure and clean formation of the desired ADC mimics, reactions with three of the top-maleimides (**MAL-27**, **MAL-78**, **MAL-83**) were repeated and analyzed by HIC, SEC (size exclusion chromatography), and MS. HIC analysis (see Scheme 6A) confirmed the formation of one main peak, putatively assigned to be DAR2, *i.e.*, a mAb conjugated to two LP mimics. SEC analysis of the samples (see SI for details) revealed small amounts of high-molecular weight (HMW) species (aggregates) in the starting material (0.6%). Upon

treatment/conjugation with **MAL-78**, no increase was observed; however, small increases to 1.1% and 1.7% HMW were observed with **MAL-27** and **MAL-83**, respectively. No increase in lower molecular-weight (LMW) species (fragment formation) was observed.

Successful conjugations of the maleimides were further confirmed by offline 2D-HIC-RPLC MS of the main peaks. The unconjugated mAb peak is shown as peak 1 in Scheme 6A. Similarly, peaks 2, 3, and 4 were assigned to the DAR2 species corresponding to **MAL-83**, **MAL-27**, and **MAL-78**, respectively (Scheme 6B). The MS values obtained are consistent with the expected values for DAR2 species.

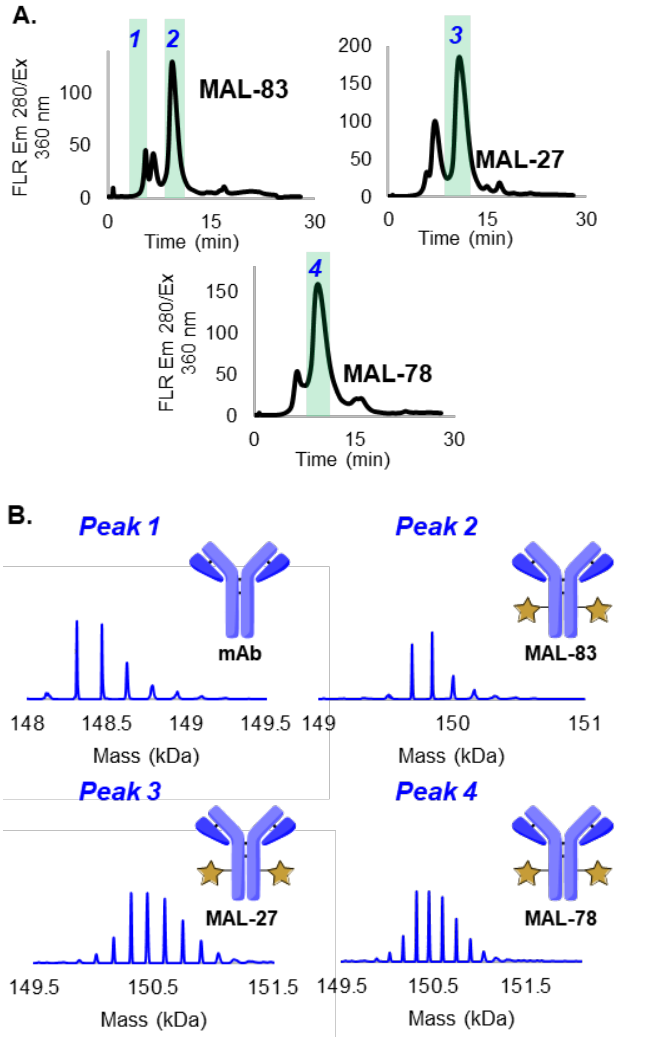

Scheme 6. MS analysis of the main peaks observed by offline 2D-HIC-RPLC-MS.

High-throughput conjugation optimization: Influence of pH and LP mimic loading on DAR. With the confirmation of key conjugate structures, we further evaluated the top maleimides in a high-throughput conjugation optimization. This experiment was designed to test whether a 3-factor optimization (LP mimic identity vs. LP mimic loading/molar equivalents vs. pH) is a useful tool to study the factors that determine success in mAb conjugations. Thus, we designed the experiment to evaluate conjugation reactivity with the seven top maleimides in 4 different loadings (2.5 to 7.8 equiv) and at two pH values (pH 5.5 and pH 7.0). The results of this experiment are shown in Scheme 7 as pie charts representing the relative area percent of the different HIC peaks. Namely, the desired DAR2 species is represented in green, DAR1 in blue, the unconjugated starting material (DAR0) in light brown, and other, unidentified protein peaks are represented in red color.

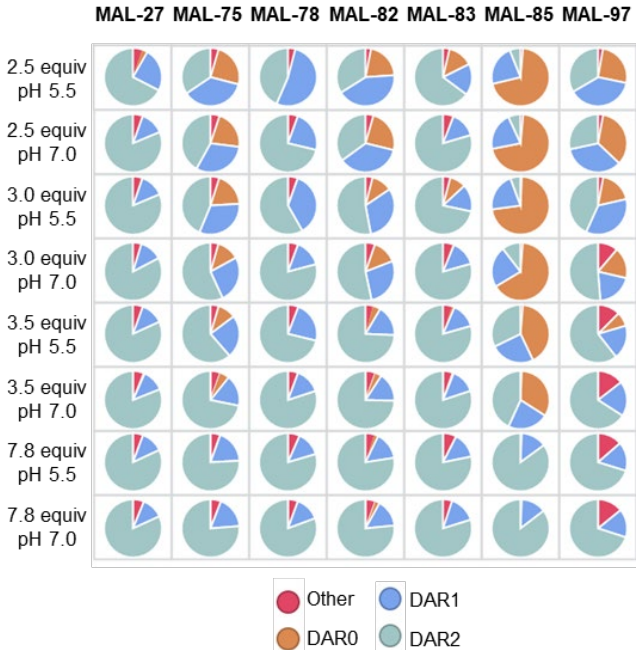

Scheme 7. Visualization of HTE conjugation data. Conditions: 10 mM histidine buffer, 15 g/L decapped thio-mAb, 2 h, 22 °C.

Analysis of these data reveals that conjugations generally proceed more readily at pH 7.0. This trend is more pronounced at lower loadings of LP mimic than at higher loadings; at 7.8 equiv, conjugation reactions are equally efficient at both tested pH values. Interestingly, the LP mimics show similar, but not identical reactivity. Again, these trends are most pronounced at lower loadings: For example, **MAL-85** is almost unreactive at 2.5 equiv; the major HIC peak in this reaction is the peak corresponding to the unconjugated DAR0 species. **MAL-27** is on the other end of the reactivity spectrum: regardless of reaction conditions, DAR2 is the main peak observed in the HIC trace. Interestingly, impurity profiles (undefined other peaks shown as red in Scheme 7) are also highly dependent on the LP mimic employed. **MAL-97** produces the largest amount of unknown side products, which likely stems from undesired reactivity of the double bond in the TCO (*trans*-cyclooctene) moiety in aqueous media. Overall, this relatively simple high-throughput experiment demonstrates the utility of LP mimics as model compounds to rapidly identify suitable conjugation reaction conditions.

Comparability of LP mimics with vcMMAE LP for thio-mAb conjugation. One of the key assumptions of maleimide conjugation chemistry is that reactions between maleimides and cysteine residues in the respective mAb are rapid and quantitative.[28-31] However, both the data presented in the last section and structure/reactivity relationships published in the literature,[32,33] suggest that the structure of the LP (mimics) can influence the DAR distribution, and thus, the quality of the ADC

(or ADC mimic in our case) obtained via conjugation. Therefore, key to the successful use of the established LP mimics would be the ability to identify the subset of LP mimics that show comparable conjugation reactivity with an actual LP of interest. For this purpose, we chose a MMAE-based LP as the reference LP since MMAE is frequently used as payload in ADCs in clinical and pre-clinical research;[34,35] and MMAE-bearing LPs are commercially available from several vendors.

For direct comparison, we chose two conjugation conditions for the MMAE LP that were already tested in the HTE optimization shown in Scheme 7. Specifically, we selected a LP loading of 3.5 or 7.8 equiv in 10 mM histidine buffer at pH 5.5. Scheme 8 graphically compares the DAR distributions obtained with the MMAE LP with the overall results obtained with the LP mimics.

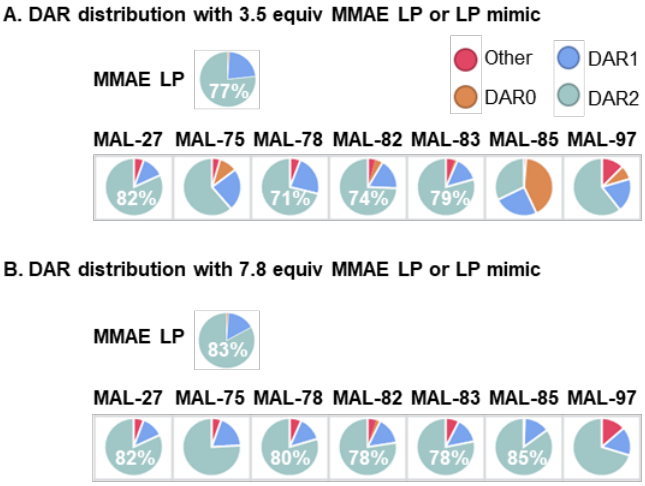

Scheme 8. Comparison of DAR distribution with LP mimics and MMAE LP. Conditions: 10 mM histidine buffer, 15 g/L decapped mAb, 22 °C. DAR2 percentage for the reactions with the MMAE LP and for LP mimics most similar to the MMAE LP are shown in the graphic.

Interestingly, higher amounts of the MMAE LP in the reaction mixture leads to an increase in DAR2 from 77% (at 3.5 equiv) to 83% (at 7.8 equiv). **MAL-78** and **MAL-82** show a similar behavior, in which the amount of DAR2 increases when the LP mimic loading is increased. Other LP mimics show relatively little change in DAR2 regardless of the loading; this is true for **MAL-27** (82% DAR2 at either loading) and **MAL-83** (79/78% at 3.5/7.8 equiv, respectively). Overall, **MAL-27**, **MAL-78**, **MAL-82**, and **MAL-83** all provide similar reactivity to the tested MMAE LP, suggesting they could be suitable replacements of a toxic LP for conjugation reaction development outside of a potent lab space. In contrast, **MAL-75**, **MAL-85**, and **MAL-97** significantly underperform in conjugation with the thio-mAb in hand. In conclusion, our studies illustrate that not each LP mimic is suitable for substituting a given LP in conjugation reaction development. Based on the HTE data shown in Scheme 8, we recommend testing a small set of maleimide candidates and compare conjugation results to those obtained with a LP of interest. This approach is likely to lead to identifying the best-suited LP mimics for a given conjugation development challenge.

LP mimics for conjugation at interchain cysteine sites. In a next step, we explored the suitability of LP mimics for visualizing the distribution of DAR species obtained from conjugation of inter-chain cysteine residues; a mAb without engineered cysteines was employed for these studies. Such cysteines are typically revealed for conjugation via reduction with TCEP (tris(2-carboxyethyl)phosphine).[36,37] We considered this study a good approach to further probe the validity of the LP mimic concept, as success for these conjugations would allow the identification of up to 9 different peaks (ranging from DAR0 to DAR8) in a HIC chromatogram.

To investigate this hypothesis, our HTE design included 4 different reduction/conjugation conditions (1.0 or 2.1 equiv TCEP; 3.0 or 4.5 equiv LP mimic; see Scheme 9); 15 reagents from the maleimide collection were used to test for conjugation. The selected maleimides included well-performing LP mimics from the studies above (*e.g.*, **MAL-27**, **MAL-83**) as well as some less HIC-shifting LP mimics (*e.g.*, **MAL-79**) as negative controls.

Selected HIC chromatograms obtained from this screen are depicted in Scheme 10 (for all HIC-chromatograms, see the SI). Excitingly, one LP mimic (**MAL-27**) shows the desired, almost statistical distribution of DAR0/2/4/6/8 peaks (Scheme 10E) with baseline resolution for all peaks.

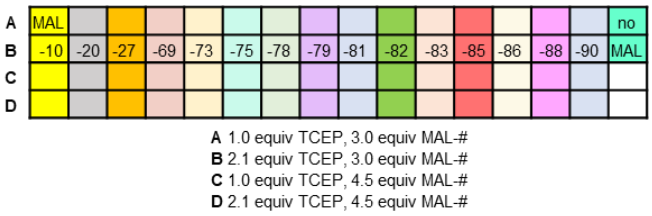

Scheme 9. Experimental design for high-throughput evaluation of LP mimics (MAL-#) in conjugation reactions with interchain cysteines. Color-shaded columns show LP mimics tested; rows indicate the screening conditions (molar equivalents of phosphine reductant TCEP and LP mimic). Conditions: 16.2 g/L mAb, pH 7.2, phosphate buffer, 22 °C, 90 min reduction time + 30 min conjugation time.

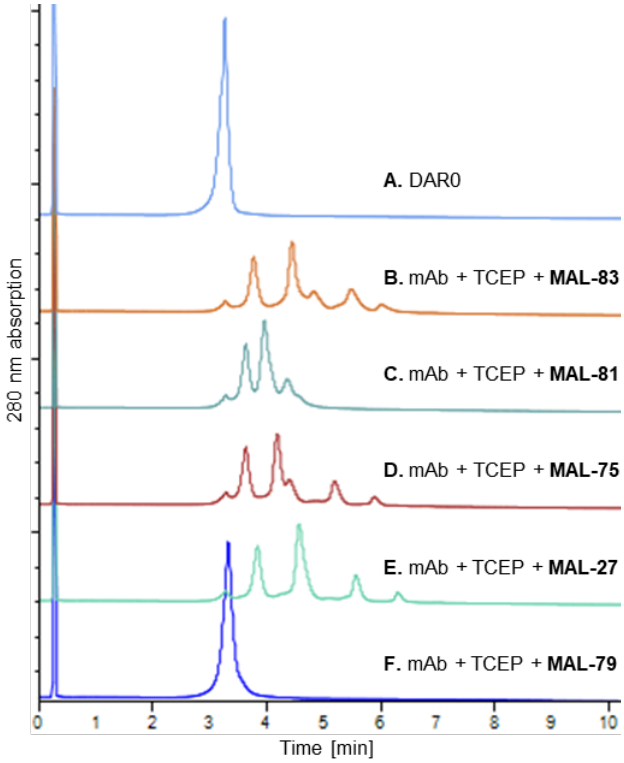

Scheme 10. Selected HIC chromatograms showing distribution of DAR0 to DAR8 species for various LP mimics. A. DAR0 peak before TCEP treatment (intact mAb). B. Peak separation including two DAR4 peaks with **MAL-83**. C. No baseline separation with **MAL-81**. D. Peak separation including two DAR4 peaks with **MAL-75**. E. Good peak separation with **MAL-27**. F. No peak separation with **MAL-79**. Conditions: phosphate buffer pH 7.2, 2.1 equiv TCEP, 22 °C, 90 min; 4.5 equiv LP mimic, 45 min.

Figure 1. Possible positional isomers for DAR4 conjugates.

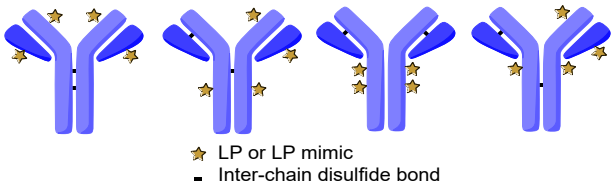

Other maleimides show similar results: Reactions with both **MAL-83** and **MAL-75** also provide HIC chromatograms with baseline-separated peaks (Scheme 10B/D). However, both chromatograms also show an additional peak right next to the DAR4 peak, which could be attributed to another DAR4 positional isomer[38] (see Figure 1); however, no further identification of these peaks was pursued. Another notable outcome is the HIC chromatogram obtained with **MAL-81**: even though the peaks are not baseline-separated, each peak is clearly visible (Scheme 10C). This finding is in agreement with **MAL-81** being a LP mimic that does not shift the HIC peaks to the same magnitude as previously observed with **MAL-27** or **MAL-83**. Finally, several LP mimics tested do not show any shift in the HIC chromatogram (*e.g.*, **MAL-79**; Scheme 10F) or show several peaks that are not identifiable, either due to peak overlap or no clear peak distribution (see the SI). Overall, **MAL-27** emerged as the best LP mimic, providing both baseline separation and a well-defined distribution of peaks. Confirmation of the identity of the observed peaks (DAR0/2/4/6/8) was performed by native SEC-MS (see the SI for details).

Having identified **MAL-27** as a suitable LP to visualize DAR distribution, we investigated the different species obtained when varying loadings of reductant (TCEP) and LP mimic. As expected, delivering substoichiometric amounts of reductant by lowering the TCEP loading from 2.1 equiv (Scheme 11B) to 1.0 equiv (Scheme 11C), resulted in DAR2 as the major conjugation species. Maintaining the TCEP loading at 2.1 equiv and decreasing the **MAL-27** loading to 3.0 equiv (Scheme 11D) results in new peaks in the HIC chromatogram. Based on their retention times, these new peaks could be odd DAR species (DAR1/3/5/7) formed due to the limited amount of **MAL-27**.

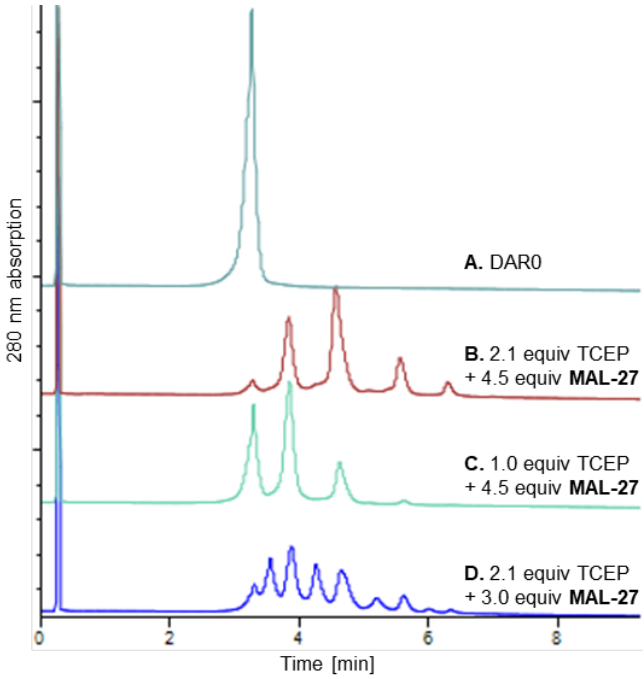

Scheme 11. Selected HIC chromatograms showing distribution of DAR0 to DAR8 species for MAL-27 conjugation after TCEP treatment under reaction conditions. A. DAR0 peak before TCEP treatment (intact mAb). B. Statistical distribution with main peak DAR4 with 2.1 equiv TCEP/4.5 equiv **MAL-27**. C. Shifted peak distribution with 1.0 equiv TCEP/ 4.5 equiv **MAL-27**. D. Additional peaks (likely DAR1/3/5/7) at low amounts of maleimides (2.1 equiv TCEP/ 3.0 equiv **MAL-27**).

Analyzing the high-throughput array of conjugation reactions (Scheme 9) by SEC (for details, see the SI) reveals that most reactions show ~98% of the main protein peak. This suggests that very few reduction/conjugation conditions lead to significant mAb aggregation or fragmentation. For **MAL-27**, the main LP of interest, this trend is true for all reaction conditions but one: Elevated fragmentation (2.7% LMW) is observed when treating the mAb with 2.1 equiv TCEP + 3.0 equiv **MAL-27**. This suggests that the lower amount **of MAL-27** in this reaction leads to fragment formation, likely via uncontrolled TCEP reduction. As TCEP and maleimides are known to react with each other,[39,40] this suggests that the excess of maleimide used in the

other reaction mixtures also prevents damage to the mAb structure by quenching the remainder of non-oxidized TCEP after the allotted reaction time.

Overall, the key takeaway from the combination of the herein described high-throughput conjugation studies is that the best LP mimics (**MAL-27**, **75**, **83**) seem to be a general solution for visualizing conjugation reactivity of MMAE-bearing mAb conjugates. This conclusion is valid across different salt gradients (NH_4OAc vs. $(NH_4)_2SO_4/K_2HPO_4$), HIC columns from different manufacturers and with different stationary phases (TSKgel Butyl-NPR vs. Sepax Proteomix Phenyl NP-1.7), and across different types of cysteines employed in conjugation (engineered vs. inter-chain cysteine sites). Based on these results, we expect that the LP mimics described herein will contribute to accelerate conjugation reaction optimizations with impacts on process, analytical, and technology development alike.

Flow conjugation in microfluidic reactors: minimizing materials requirements for conjugation optimization in flow. After considering the various types of technologies that could benefit from access to the LP mimics described above, we identified the development of continuous flow reactors for conjugation reactions as a meaningful application. In the context of ADC synthesis, continuous flow technology could offer several advantages to improve the outcome of conjugation reactions: (i) Flow reactors enable tight control of reaction parameters (*e.g.*, stoichiometry, temperature, and reaction time).[41] Thus, we hypothesized that a continuous flow conjugation may lead to improved drug/antibody ratios (DARs), and tighter DAR distribution through improved reaction control. (ii) From a process development standpoint, the implementation of a continuous flow approach for ADC conjugation would integrate well with continuous manufacturing for intensified mAb processes.[42-43 44] (iii) Finally, as a stand-alone continuous step, flow conjugation could offer additional operational advantages such as a small reactor footprint and single use reactors; both would be beneficial to facilitate the safe handling of toxic LPs.

To realize these goals, we envisioned a workflow to validate the best results obtained via HTE batch screening in a microfluidic reactor.[45] Such miniaturization would not only offer a scale-down model of a larger scale flow reactor, but also minimize the amount of mAb required for initial testing. We considered the latter an important advantage for projects with limited mAb availability, common in early development programs. Thus, we set out to design and evaluate different microfluidic mixers for conjugation. Rather than relying on commercially available yet expensive glass microchips, we chose to focus on the design and fabrication of custom-made micromixers. The decision to employ custom-made micromixers and to fabricate them in-house also enabled rapid turn-around and testing of different mixer geometries. Our goals at the outset were two-fold: (i) to identify a fabrication material compatible with mAb conjugation and (ii) to develop a micromixer geometry affording sufficient mixing of two streams at low flow rates (µL/min).

For microfluidic fabrication, the workflow we adopted involved 3D-printing of molds, followed by polydimethylsiloxane (PDMS) soft-lithography and off-ratio bonding to a glass slide (see SI for fabrication and mixing testing details).[46] Once fabrication was complete, the different micromixers were tested by flowing two colored solutions (*i.e.*, blue vs. red) through the channels at a range of desired flow rates (10 µL/min to 100 µL/min for each stream). Appearance of a uniform color after the point of mixing observed via a microscope was interpreted as a visual representation indicating sufficient mixing for a specific mixer geometry (see SI for pictures and more details).

Efficient mixing was achieved with the connected-groove mixer geometry design[47] (see SI), which was selected for subsequent flow conjugation experiments.

The flow set-up used for continuous conjugations is shown in Figure 2. It is comprised of two syringe pumps (for dispensing mAb and LP mimic solutions), capillary tubing (PTFE ID=0.01 in) connecting the micromixer to the pumps, and an additional aging coil (PTFE tubing ID=0.01 in) to reach the target residence time. Samples collected at the reactor outlet were immediately diluted and quenched prior to analysis (see experimental procedure and SI for details). Initial flow experiments were designed to compare HTE batch and microflow results employing a selection of promising LP mimics. To simplify HIC analysis, these conjugations were performed with a mAb with two engineered cysteines. An overview of selected results is depicted in Scheme 12.

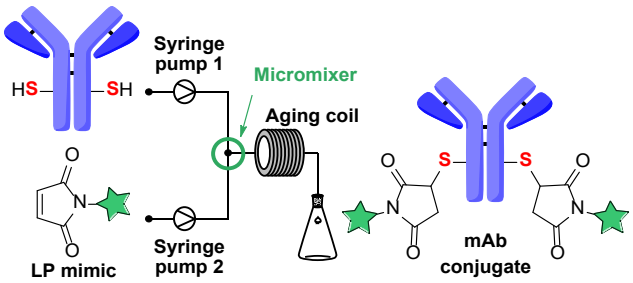

Figure 2. Microfluidic set-up for conjugation optimization.

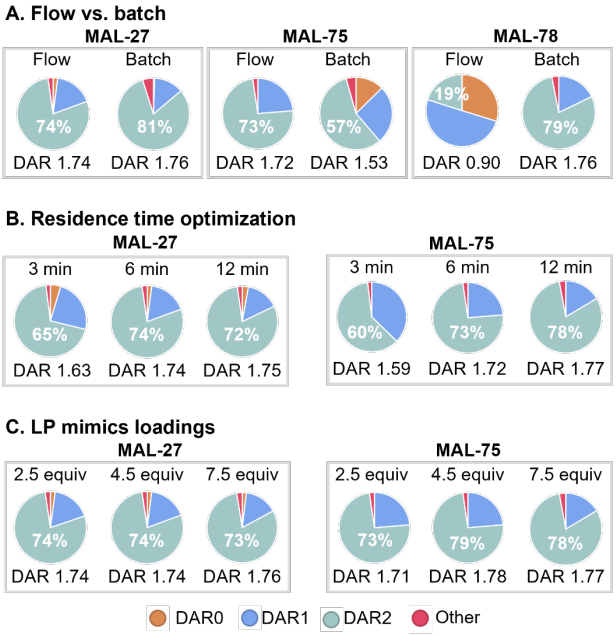

Scheme 12. Overview of continuous flow conjugation optimizations in microfluidic reactor. A. DAR% and average DAR obtained for MAL-27, MAL-75, and MAL-78; 6 min residence time, 3.5 equiv MAL. B. Residence time optimization: 3 to 12 min residence time, 3.5 equiv LP mimic. C. LP mimics loading optimization: 6 min residence time, 2.5 to 7.5 equiv LP mimics.

In Scheme 12A, the best results obtained with three different LP mimics were compared with the corresponding results obtained in batch; all flow conjugations used a 6 min residence

time. **MAL-27** showed comparable results in batch and flow (DAR 1.74 and 1.76, respectively). Conjugations with **MAL-75** resulted in an increased DAR relative to batch (DAR 1.72 vs. 1.53), while **MAL-78** yielded in worse results than in batch (DAR 0.90 vs. 1.76). We attributed the latter result to the poor stability of **MAL-78** in the buffer/DMSO mixture used for dosing this LP mimic. This hypothesis was confirmed by demonstrating that aged solutions of **MAL-78** showed either poor or no conversion, both in batcha and in flow (see SI for details). Finally, conjugations employing **MAL-83** (data not shown) demonstrate the limits of conjugations in flow: due to the poor solubility of **MAL-83** in DMSO/buffer mixtures, precipitation occurred during flow conjugation, resulting in reactor clogging.

A second round of flow optimizations focused on determining ideal residence times for the two most promising LP mimics **MAL-27** and **MAL-75**. As shown in Scheme 12B, a residence time of 6 min was found necessary to obtain high DARs for **MAL-27**. Lower DARs were observed with a 3 min residence time, while a longer residence time of 12 min showed no improvement. For **MAL-75**, an optimum residence time of 12 min resulted in a slightly improved DAR.

Finally, a range of different LP mimic loadings was evaluated with the goal to minimize the amount required for full conversion (Scheme 12C). This is an important consideration for conjugation processes, especially when using toxic LPs for ADC production: in such situations, minimizing LP loadings would result in a lower process mass intensity (PMI) and minimize the potential for exposure to toxic process intermediates. For the two different LP mimics tested here, distinctly different reactivities were obtained in this screen : Lowering the loading of **MAL-27** had only a minimal impact on reaction outcomes, with an average DAR of 1.74. This is in agreement with the data from the HTE work above (see Scheme 7), suggesting that the conjugation efficiency of **MAL-27** is maintained across a broad range of LP mimic loadings. In contrast, the results obtained with **MAL-75** show that conjugations with this LP mimic have a higher variability depending on the loadings used: the highest DAR (1.78) was obtained with at least 4.5 equiv, while lowering the loading to 2.5 equiv resulted in a DAR of 1.71. Based on these results, we ultimately selected **MAL-27** as the tool molecule for further scale-up of continuous flow conjugations.

Flow conjugation scale-up. In the next step, we translated the promising results obtained with the microfluidic set-up to a larger scale. Employing a reactor suitable for both gram scale and kg-scale processing generally offers a lower barrier for future implementation in manufacturing settings. With this goal in mind, we identified a prototype in-line static mixer offering good mixing across a broad range of flow rates and employed it to test the conjugation on 0.5 g scale.[48]. The set-up for larger scale conjugations closely resembled the microflow system; peristaltic pumps suitable for flow rates in the range of mL/min and larger diameter tubing (ID 1.60 mm, Platinum-cured Silicone tubing; see details in SI) were employed. The system was tested for continuous conjugation for an extended period of time (80 min). Slip stream samples were collected at the reactor outlet and analyzed by HIC. As depicted in Figure 4A, a consistent DAR distribution was observed throughout the experiment, highlighting the robustness of this approach. Analysis of the bulk material collected over the course of the experiment (Figure 4B) showed comparable results to what had been observed in the microfluidic scale . These data demonstrate that our initial small-scale results were reliably reproduced on a significantly larger scale (~50 x scale-up from microfluidic result to 0.5 g scale).

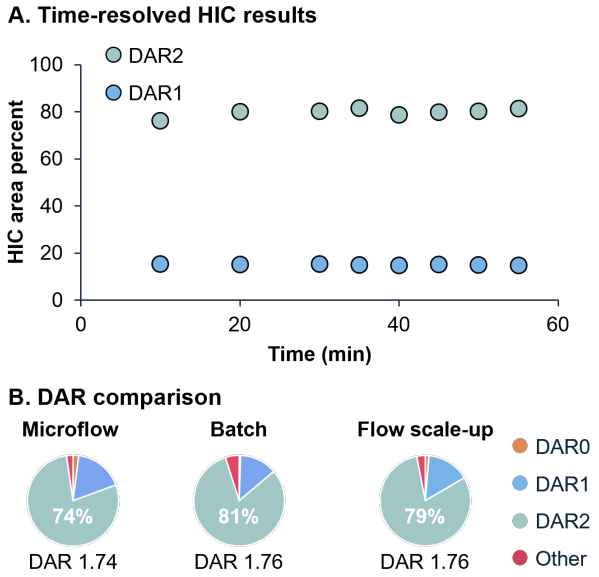

Figure 4. Flow scale-up results. A. HIC area percent of DAR1 and DAR2 from time-resolved sampling at reactor outlet during continuous flow conjugation with **MAL-27** (see experimental section for procedure details). B. Comparison of conjugation results with **MAL-27** in batch, microflow and scale-up in flow.

Summary and Conclusions

In summary, this manuscript details the identification of HIC-shifting LP mimics that allow conjugation reaction development without the use of toxic LPs, resulting in the synthesis of mAb-specific ADC mimics. Key to success was the assembly of a collection of commercially available maleimides in combination with high-throughput evaluation of their respective conjugation reactions. The herein described tool molecules allow the extensive use of high-throughput optimization for rapid identification of favorable conjugation conditions. Benchmarking the best LP mimics against a MMAE LP in conjugation with an antibody bearing two engineered cysteine residues enabled the identification of LP mimics with comparable reactivity. Additionally, the top LP mimics also visualized the statistical mixtures of DAR species obtained by the TCEP-promoted reduction of mAb interchain disulfide bonds. Finally, the non-toxic nature of the LP mimics enabled rapid technology development for conjugation. Specifically, we demonstrate the development of a microfluidic platform for flow conjugation optimization. Moreover, successful translation beyond the microfluidic scale (i.e. 0.5g of mAb) validated the initial results and highlighted the robustness and reproducibility of this approach.

Overall, we consider the work described herein to be a valuable addition to the available toolbox for conjugation reaction development. Beyond reaction optimization and continuous flow development, we anticipate that this approach will find use in the development of other technologies. For example, the maleimide collection has the potential to enable the synthesis of on-demand, diverse ADC mimics for analytical development.[11-14] Further applications in the context of continuous process development could be in the validation of separation technologies (*e.g.*, UF/DF), flow scale-up reactor design, and other aspects of initial process development requiring an understanding of ADC conjugations. In conclusion, the tools described herein provide

the opportunity to eliminate operators' exposure to toxic linker/payloads across different applications.

Experimental Procedures

Further details of reagent and mAb sourcing, synthetic and analytical equipment used, structural information of LP mimics, and all data are reported in the SI.

Conjugation HTE Screen with mAb bearing engineered cysteine residues. A 15 g/L solution of mAb with decapped engineered cysteine residues in 10 mM histidine buffer pH 5.5 was allowed to thaw (from -80 °C storage) at room temperature over 1 h. For each LP mimic, a 10.1 mM solution in dimethylsulfoxide was prepared. 10 µL (corresponding to 0.101 µmol, 10 equiv) of maleimide solution was added to the appropriate well of a 96-well plate (for 2D screen design details, see the SI). Then, 100 µL of the mAb stock solution (corresponding to 0.0101 µmol, 1.0 equiv) was added to each well. Reactions were sampled after 1 and 18 h. For HIC analysis, 45 µL of reaction solution was diluted to 500 µL with 10 mM histidine buffer pH 5.5. 6 µL of the resulting solution (corresponding to 10 µg) were injected onto a HIC column (Sepax Proteomix Phenyl NP-1.7 4.6 x 100 mm, 1.7 µm); analysis was performed with a gradient of 85% mobile phase A (3.0 M NH_4OAc with 50 mM K_2HPO_4, pH 7.0, 5% acetonitrile)/15% mobile phase B (5% acetonitrile) to 25 % A/ 75% B (column temperature 35 °C, see SI for further method details). Peak detection was performed at 280 nm; high-throughput visualization and integration was performed using Virscidian Analytical Studio Professional.

3-Factor HTE with mAb bearing engineered cysteine residues: LP mimics, LP mimic equivalents, pH. 17.8 mM stock solutions of LP mimics in dimethylsulfoxide were prepared. The decapped mAb solution (15 g/L in 10 mM histidine, pH 5.5) was allowed to thaw (from -80 °C storage) at room temperature over 1 h. A 0.75 M Na_3PO_4 solution was prepared and filtered through a 0.2 µm filter. The mAb stock solution was divided equally into two vials. One part of the solution was used directly for screening; the other was adjusted to pH 7.0 with a Na_3PO_4 solution . The maleimide solutions (2.9 to 8.9 µL; 0.0516 µmol to 0.1584 µmol; 2.54 to 7.80 equiv maleimide) were added to the high-throughput plate first, followed by addition of 200 µL (corresponding to 0.0203 µmol; 1.0 equiv) of decapped mAb solution (pH 5.5 or pH 7.0). The reactions were placed onto a shaker (300 rpm, 22 °C) for 18 h and analyzed by HIC, employing the same method described in the conjugation HTE procedure (see also SI for further method details.)

3-Factor HTE with mAb to conjugate inter-chain cysteine residues: LP mimics, LP mimic loading, TCEP loading. 9.0 mM stock solutions of maleimides in N,N-dimethyl acetamide were prepared. Solutions were stored at 5 °C for 2 h until use. A 5.0 mM stock solution of tris(2-carboxyethyl)phosphine hydrochloride (TCEP) in water was prepared. A 40.6 g/L solution of mAb in 15 mM acetate buffer, 5% (w/v) sucrose, 0.02% (w/v) Polysorbate-80 (PS80), pH 5.2 was removed from the -80 °C freezer and allowed to warm to room temperature over 1 h. 4.0 mL of this solution was diluted with 6.0 mL 48 mM phosphate buffer (pH 8.05, 2.67 mM EDTA disodium). The resulting solution was pH adjusted to pH 7.2 with 1 M AcOH solution. The solution was then split into two vials (5.00 mL, 0.5491 µmol, 1.00 equiv mAb per vial). 108.5 µL (0.5425 µmol, 1.0 equiv) or 232.8 µL (1.164 µmol, 2.12 equiv) TCEP stock solution was added to the respective vial. The mixtures were shaken gently (300 rpm, 22 °C; Eppendorf ThermoMixer® C) for 90 min. Maleimide stock solutions (3.5 µL to 5.3 µL; 0.0315 µmol to 0.0477 µmol; 3.0 to 4.5 equiv) were dispensed into a 96 well plate. After the reduction reaction time was complete (90 min), 100 µL of the reduction reaction solutions (corresponding to 0.0107 µmol mAb) were dispensed across the conjugation plate as required by the HTE design. The conjugation reaction mixtures were shaken gently (300 rpm, 22 °C) for 30 min. After the conjugation reaction time was completed, the mixtures were added to a quench plate containing 300 µL 10 mM histidine buffer pH 5.5 and 2.3 µL 1 M AcOH solution per well. 12 µL of the resulting solutions (46.5 µg) were injected for HIC analysis. 7 µL of the resulting solutions (27 µg) were injected for SEC analysis. For details on the methods used for HIC and SEC analysis, see the SI.

Conjugation with mAb bearing engineered cysteine residues in a microfluidic flow reactor. A 15 g/L (0.1011 mM) solution of mAb with decapped engineered cysteine residues in 10 mM histidine buffer pH 5.5 was allowed to thaw (from -80 °C storage) at room temperature over 1 h. The mAb solution pH was adjusted to 7.0 by addition of 1.25 M Na_3PO_4. For each maleimide to be tested, a solution in water/DMSO 9:1 was prepared by weighing the desired amount of LP mimic and dissolving in DMSO first, followed by slow addition of water. The LP mimic solution concentration was selected in order to afford a MAL loading of 2.5, 3.5, 4.5 or 7.5 equivalents when flowing at a 1:1 flow ratio relative to the mAb. For example, for 3.5 equiv **MAL-27**, a 0.3538 mM solution in water/DMSO 9:1 was prepared. The mAb and LP mimic solutions were used as-is and flowed through the micromixer and aging coil at a flow rate of 30 µL/min each (60 µL/min total flow rate). Given the reactor volume of 360 µL, this flow rate corresponded to a residence time of 6 minutes. Upon exiting the reactor, 100 µL of reaction mixture (1 min 40 sec collection time) were collected in a vial containing 350 µL of pH 5.5 10 mM His buffer and 5 µL of 1 M AcOH to quench reaction. Analysis via HIC chromatography (5 µL/12 µg injection) was performed with the same method described above for batch experiments (see also SI for further method details).

Conjugation with mAb bearing engineered cysteine residues in a larger flow reactor. A 15 g/L (0.1011 mM, 25 mL) solution of mAb with decapped engineered cysteine residues in 10 mM histidine buffer pH 5.5 was allowed to thaw (from -80 °C storage) at room temperature over 1 h. The mAb solution pH was adjusted to 7.0 by addition of 1.25 M Na_3PO_4. A solution of **MAL-27** in water/DMSO 9:1 was prepared by weighing 16 mg into a volumetric flask. **MAL-27** was dissolved in 5 mL of DMSO, followed by slow addition of pH 7 10 mM His buffer to a total volume of 50 mL (0.303 M). To maximize solution stability of the LP mimics in buffer/DMSO mixtures, the addition of buffer to reach the desired volume was done immediately before the start of the flow experiment. Both solutions were flowed through the mixer and aging coil at a flow rate of 0.428 mL/min each (0.857 mL/min total flow rate). Given the total reactor volume of 6.27 mL post mixing, this flow rate corresponded to a residence time of 7 minutes. During flow operation, the outcoming stream was discarded to waste for the first 10 min to allow for system equilibration and then collected in a new fraction in 5 min increments for a total flow time of 70 min. In addition, samples of 300 µL of reaction mixture (21 sec collection time) were taken at regular intervals of 10 or 5 minutes. These samples were diluted with 1050 µL of pH 5.5 10 mM His buffer and 15 µL of 1 M AcOH as reaction quench. Analysis via HIC chromatography (5 µL/12 µg injection) was performed with the same method described above for batch experiments.

ASSOCIATED CONTENT

Supporting Information

Details of analytical methods, collection build workflow, conjugation reaction procedures, HIC, SEC, and MS data, HTE plate designs, flow reactor designs. The Supporting Information is available free of charge on the ACS Publications website.

AUTHOR INFORMATION

Corresponding Authors

*marion.emmert@merck.com, *cecilia.bottecchia@merck.com

ACKNOWLEDGMENT

The authors acknowledge Mark Brower, Lara Fernandez-Cerezo, Ian Mangion, Jeff Moore, Hong Ren, and Michelle Wong (all Merck & Co, Inc) for helpful discussions.

REFERENCES

(1) Chia, C. S. B., A Patent Review on FDA-Approved Antibody-Drug Conjugates, Their Linkers and Drug Payloads. *ChemMedChem* **2022,** *17* (11), e202200032.

(2) Gogia, P.; Ashraf, H.; Bhasin, S.; Xu, Y., Antibody Drug Conjugates: A Review of Approved Drugs and Their Clinical Level of Evidence. *Cancers* **2023,** *15* (15), 3886.

(3) Bajjuri, K. M.; Liu, Y.; Liu, C.; Sinha, S. C., The legumain protease-activated auristatin prodrugs suppress tumor growth and metastasis without toxicity. *ChemMedChem* **2011,** *6* (1), 54-9.

(4) Fisher, J. E., Jr., Considerations for the Nonclinical Safety Evaluation of Antibody-Drug Conjugates. *Antibodies (Basel)* **2021,** *10* (2).

(5) Masters, J. C.; Nickens, D. J.; Xuan, D.; Shazer, R. L.; Amantea, M., Clinical toxicity of antibody drug conjugates: a meta-analysis of payloads. *Invest New Drugs* **2018,** *36* (1), 121-135.

(6) Modi, S.; Jacot, W.; Yamashita, T.; Sohn, J.; Vidal, M.; Tokunaga, E.; Tsurutani, J.; Ueno, N. T.; Chae, Y. S.; Lee, K. S.; Niikura, N.; Park, Y. H.; Wang, X.; Xu, B.; Gambhire, D.; Yung, L.; Meinhardt, G.; Wang, Y.; Harbeck, N.; Cameron, D. A., Trastuzumab deruxtecan (T-DXd) versus treatment of physician's choice (TPC) in patients (pts) with HER2-low unresectable and/or metastatic breast cancer (mBC): Results of DESTINY-Breast04, a randomized, phase 3 study. *Journal of Clinical Oncology* **2022,** *40* (17_suppl), LBA3-LBA3.

(7) Professional Committee on Clinical Research of Oncology Drugs, C. A.-C. A.; Expert Committee for Monitoring the Clinical Application of Antitumor, D.; Breast Cancer Expert Committee of National Cancer Quality Control, C.; Cancer Chemotherapy Quality Control Expert Committee of Beijing Cancer Treatment Quality, C.; Improvement, C., Expert consensus on the clinical application of antibody-drug conjugates in the treatment of malignant tumors (2021 edition). *Cancer Innovation* **2022,** *1* (1), 3-24.

(8) Hu, X.; Bortell, E.; Kotch, F. W.; Xu, A.; Arve, B.; Freese, S., Development of Commercial-Ready Processes for Antibody Drug Conjugates. *Organic Process Research & Development* **2017,** *21* (4), 601-610.

(9) Graham, J. C.; Hillegass, J.; Schulze, G., Considerations for setting occupational exposure limits for novel pharmaceutical modalities. *Regul Toxicol Pharmacol* **2020,** *118*, 104813.

(10) Silva, T. C.; Eppink, M.; Ottens, M., Automation and miniaturization: enabling tools for fast, high-throughput process development in integrated continuous biomanufacturing. *Journal of Chemical Technology & Biotechnology* **2021,** *97* (9), 2365-2375.

(11) Birdsall, R. E.; Shion, H.; Kotch, F. W.; Xu, A.; Porter, T. J.; Chen, W., A rapid on-line method for mass spectrometric confirmation of a cysteine-conjugated antibody-drug-conjugate structure using multidimensional chromatography. *MAbs* **2015,** *7* (6), 1036-44.

(12) Wang, J.; Zhang, W.; Salter, R.; Lim, H. K., Reductive Desulfuration as an Important Tool in Detection of Small Molecule Modifications to Payload of Antibody Drug Conjugates. *Anal Chem* **2019,** *91* (3), 2368-2375.

(13) Yan, Y.; Xing, T.; Wang, S.; Daly, T. J.; Li, N., Online coupling of analytical hydrophobic interaction chromatography with native mass spectrometry for the characterization of monoclonal antibodies and related products. *J Pharm Biomed Anal* **2020,** *186*, 113313.

(14) Achanta, P. S.; Friesen, J. B.; Harris, G.; Webster, G. K.; Chen, S. N.; Pauli, G. F., Development of Centrifugal Partition Chromatography for the Purification of Antibody-Drug Conjugates. *Anal Chem* **2023,** *95* (5), 2783-2788.

(15) Barrientos, R.C.; Losacco, G.L.; Azizi, M.; Wang, H.; Nguyen, A.N.; Shchurik, V.; Singh, A.; Richardson, D.; Mangion, I.; Guillarme, D.; Regalado, E.L.; Haidar Ahmad, I.A. Automated Hydrophobic Interaction Chromatography Screening Combined with In Silico Optimization as a Framework for Nondenaturing Analysis and Purification of Biopharmaceuticals. *Anal. Chem.* **2022**, *94*, 49, 17131–17141.

(16) Liu, T.; Tao, Y.; Xia, X.; Zhang, Y.; Deng, R.; Wang, Y., Analytical tools for antibody–drug conjugates: From in vitro to in vivo. *TrAC Trends in Analytical Chemistry* **2022,** *152*.

(17) Matsuda, Y.; Mendelsohn, B. A., Recent Advances in Drug-Antibody Ratio Determination of Antibody-Drug Conjugates. *Chem Pharm Bull (Tokyo)* **2021,** *69* (10), 976-983.

(18) D'Atri, V.; Pell, R.; Clarke, A.; Guillarme, D.; Fekete, S., Is hydrophobic interaction chromatography the most suitable technique to characterize site-specific antibody-drug conjugates? *J Chromatogr A* **2019,** *1586*, 149-153.

(19) Kallsten, M.; Hartmann, R.; Artemenko, K.; Lind, S. B.; Lehmann, F.; Bergquist, J., Qualitative analysis of antibody-drug conjugates (ADCs): an experimental comparison of analytical techniques of cysteine-linked ADCs. *Analyst* **2018,** *143* (22), 5487-5496.

(20) Ouyang, J., Drug-to-antibody ratio (DAR) and drug load distribution by hydrophobic interaction chromatography and reversed phase high-performance liquid chromatography. *Methods Mol Biol* **2013,** *1045*, 275-83.

(**Error! Bookmark not defined.**) Colombo, R.; Rich, J. R., The therapeutic window of antibody drug conjugates: A dogma in need of revision. *Cancer Cell* **2022,** *40* (11), 1255-1263.

(21) Junutula, J. R.; Raab, H.; Clark, S.; Bhakta, S.; Leipold, D. D.; Weir, S.; Chen, Y.; Simpson, M.; Tsai, S. P.; Dennis, M. S.; Lu, Y.; Meng, Y. G.; Ng, C.; Yang, J.; Lee, C. C.; Duenas, E.; Gorrell, J.; Katta, V.; Kim, A.; McDorman, K.; Flagella, K.; Venook, R.; Ross, S.; Spencer, S. D.; Lee Wong, W.; Lowman, H. B.; Vandlen, R.; Sliwkowski, M. X.; Scheller, R. H.; Polakis, P.; Mallet, W., Site-specific conjugation of a cytotoxic drug to an antibody improves the therapeutic index. *Nat Biotechnol* **2008,** *26* (8), 925-32.

(22) Junutula, J. R.; Flagella, K. M.; Graham, R. A.; Parsons, K. L.; Ha, E.; Raab, H.; Bhakta, S.; Nguyen, T.; Dugger, D. L.; Li, G., Engineered thio-trastuzumab-DM1 conjugate with an improved therapeutic index to target human epidermal growth factor receptor 2–positive breast cancer. *Clinical cancer research* **2010,** *16* (19), 4769-4778.

(23) Ohri, R.; Bhakta, S.; Fourie-O'Donohue, A.; Dela Cruz-Chuh, J.; Tsai, S. P.; Cook, R.; Wei, B.; Ng, C.; Wong, A. W.; Bos, A. B.; Farahi, F.; Bhakta, J.; Pillow, T. H.; Raab, H.; Vandlen, R.; Polakis, P.; Liu, Y.; Erickson, H.; Junutula, J. R.; Kozak, K. R., High-Throughput Cysteine Scanning To Identify Stable Antibody Conjugation Sites for Maleimide- and Disulfide-Based Linkers. *Bioconjug Chem* **2018,** *29* (2), 473-485.

(24) Behrens, C. R.; Ha, E. H.; Chinn, L. L.; Bowers, S.; Probst, G.; Fitch-Bruhns, M.; Monteon, J.; Valdiosera, A.; Bermudez, A.; Liao-Chan, S.; Wong, T.; Melnick, J.; Theunissen, J. W.; Flory, M. R.; Houser, D.; Venstrom, K.; Levashova, Z.; Sauer, P.; Migone, T. S.; van der Horst, E. H.; Halcomb, R. L.; Jackson, D. Y., Antibody-Drug Conjugates (ADCs) Derived from Interchain Cysteine Cross-Linking Demonstrate Improved Homogeneity and Other Pharmacological Properties over Conventional Heterogeneous ADCs. *Mol Pharm* **2015,** *12* (11), 3986-98.

(25) You, J.; Zhang, J.; Wang, J.; Jin, M., Cysteine-Based Coupling: Challenges and Solutions. *Bioconjug Chem* **2021,** *32* (8), 1525-1534.

(26) Chang, P. V.; Prescher, J. A.; Sletten, E. M.; Baskin, J. M.; Miller, I. A.; Agard, N. J.; Lo, A.; Bertozzi, C. R., Copper-free click chemistry in living animals. *Proceedings of the National Academy of Sciences of the United States of America* **2010,** *107*, 1821–1826.

(27) Neves, A. A.; Stöckmann, H.; Wainman, Y. A.; Kuo, J. C. H.; Fawcett, S.; Leeper, F. J.; Brindle, K. M., Imaging Cell Surface Glycosylation in Vivo Using "Double Click" Chemistry. *Bioconjugate Chemistry* **2013,** *24* (6), 934-941.

(28) Schelté, P.; Boeckler, C.; Frisch, B.; Schuber, F., Differential Reactivity of Maleimide and Bromoacetyl Functions with Thiols: Application to the Preparation of Liposomal Diepitope Constructs. *Bioconjugate Chemistry* **2000,** *11* (1), 118-123.

(29) McConnell, E. W.; Smythers, A. L.; Hicks, L. M., Maleimide-Based Chemical Proteomics for Quantitative Analysis of Cysteine Reactivity. *Journal of the American Society for Mass Spectrometry* **2020,** *31* (8), 1697-1705.

(30) Vanderhooft, J. L.; Mann, B. K.; Prestwich, G. D., Synthesis and Characterization of Novel Thiol-Reactive Poly(ethylene glycol) Cross-Linkers for Extracellular-Matrix-Mimetic Biomaterials. *Biomacromolecules* **2007,** *8* (9), 2883-2889.

(31) Bednar, R. A., Reactivity and pH dependence of thiol conjugation to N-ethylmaleimide: detection of a conformational change in chalcone isomerase. *Biochemistry* **1990,** *29* (15), 3684-3690.

(32) Feuillâtre, O.; Gély, C.; Huvelle, S.; Baltus, C. B.; Juen, L.; Joubert, N.; Desgranges, A.; Viaud-Massuard, M.-C.; Martin, C., Impact of Maleimide Disubstitution on Chemical and Biological Characteristics of HER2 Antibody–Drug Conjugates. *ACS Omega* **2020,** *5* (3), 1557-1565.

(33) Christie, R. J.; Fleming, R.; Bezabeh, B.; Woods, R.; Mao, S.; Harper, J.; Joseph, A.; Wang, Q.; Xu, Z.-Q.; Wu, H.; Gao, C.; Dimasi, N., Stabilization of cysteine-linked antibody drug conjugates with N-aryl maleimides. *Journal of Controlled Release* **2015,** *220*, 660-670.

(34) Li, H.; Li, H., A narrative review of the current landscape and future perspectives of HER2-targeting antibody drug conjugates for advanced breast cancer. *Translational Breast Cancer Research* **2021,** *2*.

(35) Singh, D.; Dheer, D.; Samykutty, A.; Shankar, R., Antibody drug conjugates in gastrointestinal cancer: From lab to clinical development. *Journal of Controlled Release* **2021,** *340*, 1-34.

(36) Liu-Shin, L.; Fung, A.; Malhotra, A.; Ratnaswamy, G., Influence of disulfide bond isoforms on drug conjugation sites in cysteine-linked IgG2 antibody-drug conjugates. *MAbs* **2018,** *10* (4), 583-595.

(37) Chiang, Z. C.; Chiu, Y. K.; Lee, C. C.; Hsu, N. S.; Tsou, Y. L.; Chen, H. S.; Hsu, H. R.; Yang, T. J.; Yang, A. S.; Wang, A. H., Preparation and characterization of antibody-drug conjugates acting on HER2-positive cancer cells. *PLoS One* **2020,** *15* (9), e0239813.

(38) Chen, H.; Qiu, D.; Shi, J.; Wang, N.; Li, M.; Wu, Y.; Tian, Y.; Bu, X.; Liu, Q.; Jiang, Y.; Hamilton, S. E.; Han, P.; Sun, S., In-Depth Structure and Function Characterization of Heterogeneous Interchain Cysteine-Conjugated Antibody–Drug Conjugates. *ACS Pharmacology & Translational Science* **2024,** *7* (1), 212-221.

(39) Kantner, T.; Alkhawaja, B.; Watts, A. G., In Situ Quenching of Trialkylphosphine Reducing Agents Using Water-Soluble PEG-Azides Improves Maleimide Conjugation to Proteins. *ACS Omega* **2017,** *2* (9), 5785-5791.

(40) Kantner, T.; Alkhawaja, B.; Watts, A. G., In Situ Quenching of Trialkylphosphine Reducing Agents Using Water-Soluble PEG-Azides Improves Maleimide Conjugation to Proteins. *ACS Omega* **2017,** *2* (9), 5785-5791.

(41) Nakahara, Y.; Mendelsohn, B. A.; Matsuda, Y., Antibody–Drug Conjugate Synthesis Using Continuous Flow Microreactor Technology. *Organic Process Research & Development* **2022,** *26* (9), 2766-2770.

(42) Somasundaram, B.; Pleitt, K.; Shave, E.; Baker, K.; Lua, L. H. L., Progression of continuous downstream processing of monoclonal antibodies: Current trends and challenges. *Biotechnology and Bioengineering* **2018,** *115* (12), 2893-2907.

(43) Zydney, A. L., Continuous downstream processing for high value biological products: A Review. *Biotechnology and Bioengineering* **2016,** *113* (3), 465-475.

(44) Gupta, P.; Kateja, N.; Mishra, S.; Kaur, H.; Rathore, A. S., Economic assessment of continuous processing for manufacturing of biotherapeutics. Biotechnology Progress 2021, 37 (2), e3108.

(45) Endo, Y.; Nakahara, Y.; Shiroma, R.; Takimoto, K.; Matsuda, Y., Development and Characterization of a Portable Flow Microreactor for Enhanced Bioconjugation Applications. *Organic Process Research & Development* **2024**, DOI: 10.1021/acs.oprd.3c00384.

(46) Bhattacharjee, N.; Urrios, A.; Kang, S.; Folch, A., The upcoming 3D-printing revolution in microfluidics. *Lab on a Chip* **2016,** *16* (10), 1720-1742.

(47) Yang, J.-T.; Fang, W.-F.; Tung, K.-Y., Fluids mixing in devices with connected-groove channels. *Chemical Engineering Science* **2008,** *63* (7), 1871-1881.

(48) The prototype in-line static mixer used for this evaluation was provided, designed and owned by Merck KGaA, Darmstadt, Germany and/or its affiliates.

Table of Contents artwork